NIH Public Access
Author Manuscript
Mol Cell Neurosci. Author manuscript; available in PMC 2012 June 1.

Published in final edited form as:
Mol Cell Neurosci. 2011 June ; 47(2): 154–165. doi:10.1016/j.mcn.2011.04.001.

Site-specific hyperphosphorylation of pRb in HIV-induced neurotoxicity

C. Akay[1], **K.A. Lindl**[1], **Y. Wang**[1], **M.G. White**[1], **J Isaacman-Beck**[2], **D.L. Kolson**[2], and **K.L. Jordan-Sciutto**[*,1]

[1]Department of Pathology, School of Dental Medicine, University of Pennsylvania, Philadelphia, PA, 19104

[2]Department of Neurology, School of Medicine, University of Pennsylvania, Philadelphia, PA 19104

Abstract

HIV-Associated Neurocognitive Disorder (HAND) remains a serious complication of HIV infection, despite combination anti-retroviral therapy. Neuronal dysfunction and death is attributed to soluble factors released from activated and/or HIV-infected macrophages. Most of these factors affect the cell cycle machinery, determining cellular outcomes even in the absence of cell division. One of the earliest events in cell cycle activation is hyperphosphorylation of the retinoblastoma protein, pRb (ppRb). We and others have previously shown increased expression of ppRb in the CNS of patients with HIV encephalitis (HIVE) and in neurons in an *in vitro* model of HIV-induced neurodegeneration. However, trophic factors also lead to an increase in neuronal ppRb with an absence of cell death, suggesting that, depending on the stimulus, hyperphosphorylation of pRb can have different outcomes on neuronal fate. pRb has multiple serines and threonines targeted for phosphorylation by distinct kinases, and we hypothesized that different stimuli may target separate sites for phosphorylation. Thus, to determine whether pRb is differentially phosphorylated in response to different stimuli and whether any of these sites is preferentially phosphorylated in association with HIV-induced neurotoxicity, we treated primary rat mixed cortical cultures with trophic factors, BDNF or RANTES, or with the neurotoxic factor, N-methyl-D-aspartate (NMDA), or with supernatants containing factors secreted by HIV-infected monocyte-derived macrophages (HIV-MDM), our *in vitro* model of HIV-induced neurodegeneration. We found that, while BDNF and RANTES phosphorylated serine807/811 and serine608 *in vitro*, treatment with HIV-MDM did not, even though these trophic factors are components of HIV-MDM. Rather, HIV-MDM targets a specific phosphorylation site, serine795, of pRb for phosphorylation *in vitro* and this ppRb isoform is also increased in HIV-infected brains *in vivo*. Further, overexpression of a nonphosphorylatable pRb (ppRb S795A) attenuated HIV-MDM-induced neurotoxicity. These findings indicate that HIV-infection in the brain is associated with site-specific hyperphosphoylation of pRb at serine795, which is not induced by other tested stimuli, and that this phosphorylation contributes to neuronal death in this disease, demonstrating that specific pRb sites are differentially targeted and may have diverse impacts on the viability of post-mitotic neurons.

© 2011 Elsevier Inc. All rights reserved.

[*]Corresponding Author: Kelly L. Jordan-Sciutto, Ph.D., Department of Pathology, University of Pennsylvania, 240 S. 40th St, Rm 312 Levy Bldg, Philadelphia, PA 19104-6030, jordank@upenn.edu, phone: 215-898-4196, fax: 215-573-2050.

Publisher's Disclaimer: This is a PDF file of an unedited manuscript that has been accepted for publication. As a service to our customers we are providing this early version of the manuscript. The manuscript will undergo copyediting, typesetting, and review of the resulting proof before it is published in its final citable form. Please note that during the production process errors may be discovered which could affect the content, and all legal disclaimers that apply to the journal pertain.

NIH-PA Author Manuscript
NIH-PA Author Manuscript
NIH-PA Author Manuscript

NIH-PA Author Manuscript

NIH-PA Author Manuscript

NIH-PA Author Manuscript

Keywords

Retinoblastoma; HIV-associated neurocognitive disorder; cyclin-dependent kinase; cyclin-dependent kinase 5; neurotrophins; chemokines

1. Introduction:

In the Central Nervous System (CNS), HIV manifests itself clinically as HIV-Associated Neurocognitive Disorder (HAND), which is estimated to affect 50% of the HIV(+) population in the current era of combined Anti-Retroviral Therapy (cART) (Dore et al., 1999; Heaton et al., 2010; Masliah et al., 2000; McArthur, 2004; Neuenburg et al., 2002). The neurological manifestations of HAND encompass a multitude of cognitive, behavioral, and motor deficits of varying severity (McArthur, 2004; Navia et al., 1986; Portegies et al., 1993; Woods et al., 2009). While the incidence of the most severe forms of HAND has decreased significantly with the widespread use of cART, subtler forms of HAND have become more prevalent (Heaton et al., 2010). Interestingly, there is little evidence supporting direct infection of neurons by HIV. Rather, culminating data support a model whereby HIV crosses the blood-brain barrier via infected monocytes that differentiate into macrophages and establishes a persistent infection within macrophages/microglia (M/M), creating a viral reservoir within the brain (Gendelman et al., 1994; Gonzalez-Scarano and Martin-Garcia, 2005a). These infected/activated M/M alter the extracellular environment by releasing numerous soluble factors, including viral proteins, cytokines, chemokines, quinolinic acid, TNF-α, and reactive oxygen species, which results in release of more of these and other neurotoxic and pro-inflammatory factors from astrocytes, neurons, and microglia (Giulian et al., 1996; Power and Johnson, 1995; Price et al., 1988; Soontornniyomkij et al., 1998). On the other hand, non-toxic trophic factors are also released into the extracellular milieu, potentially in an attempt to overcome the onslaught of toxic factors (Soontornniyomkij et al., 1998). Ultimately, with the progression of disease, the ensuing neuroinflammation disrupts neuronal function and leads to neuronal death. Importantly, *in vivo* studies have mirrored findings *in vitro*, showing an increase of both neurotoxic (e.g. TNF-α, MCP-1, IL-6) (Achim et al., 1996; Conant et al., 1998; Gisolf et al., 2000; Sippy et al., 1995) and neurotrophic (e.g. MIP-1α, FGF, BDNF) (Everall et al., 2001; Nuovo and Alfieri, 1996; Soontornniyomkij et al., 1998) factors in the cerebrospinal fluid (CSF) of HIV-infected patients. The precise mechanisms by which neuronal death occurs in response to this functionally diverse group of factors remain only partially defined; however, several mechanisms, including NMDA receptor stimulation (O'Donnell et al., 2006; Wang et al., 2007), calcium influx (Galicia et al., 2002), caspase and/or calpain activation (Wang et al., 2007), activation of p38 mitogen activated protein kinase (MAPK) and PI3K/Akt pathways (Ullrich et al., 2000), and/or aberrant cell cycle regulation (Jordan-Sciutto et al., 2002b) are suggested as determinants of neuronal viability in HAND. Interestingly, several neurodegenerative disorders, such as Alzheimer Disease (AD), Parkinson Disease (PD), Amyotrophic Lateral Sclerosis (ALS), and HAND, display increased and/or altered expression of various cell cycle proteins in neurons, suggesting that cell cycle proteins may play important roles in determination of neuronal fate in disease (Jordan-Sciutto et al., 2001; Jordan-Sciutto et al., 2003; Jordan-Sciutto et al., 2002a; Jordan-Sciutto et al., 2002b; Jordan-Sciutto et al., 2000; Ranganathan and Bowser, 2003; Wang et al., 2010).

Retinoblastoma protein (pRb) is a key cell cycle regulator with the ability to target diverse signaling pathways and is therefore a major contributor to decisions about whether a cell divides, differentiates, senesces or dies (Harbour and Dean, 2000a, b). One of the essential events in cell cycle activation is hyperphosphorylation of pRb (ppRb) during the G1 phase of the cell cycle. In dividing cells, pRb prevents quiescent cells from entering the cell cycle

NIH-PA Author Manuscript

NIH-PA Author Manuscript

NIH-PA Author Manuscript

through its repression of the transcriptional activity of cell cycle protein, E2F1 (Frolov and Dyson, 2004). The interaction between pRb and E2F1 and between pRb and other members of the E2F family of transcription factors is regulated by phosphorylation of pRb via CyclinD:cyclin dependent kinase (CDK)4, cyclinD:CDK6, or cyclin E:CDK2 complexes. pRb phosphorylation by one or more of CDKs abrogates pRb-mediated repression of the E2F family of transcription factors, leading to transactivation of a myriad of E2F target genes, including those necessary for DNA synthesis and S-phase progression, as well as those that induce cell death (DeGregori et al., 1997; Hallstrom and Nevins, 2003).

pRb is enriched in serines and threonines and is predicted to have over 30 potential phosphorylation sites, at least 12 of which are known to be phosphorylated *in vivo* (Connell-Crowley et al., 1997; Hamel et al., 1990; Kitagawa et al., 1996; Knudsen and Wang, 1996, 1997; Lees et al., 1991; Lin et al., 1991; Zarkowska and Mittnacht, 1997). While pRb phosphorylation at serine795 mainly regulates the disruption of the pRb:E2F1 complex, phosphorylation at serine807 and serine811 are involved in c-abl binding, and threonine821 and threonine826 have been shown to regulate binding to LxCxE-containing proteins (Knudsen and Wang, 1996). On the other hand, phosphorylation of pRb serine608 by Check point kinase (Chk) 1/2, in response to DNA damage, actually leads to complex formation with E2F1 (Inoue et al., 2007). Further, a recent report shows that pRb phosphorylation at threonine356/373 inhibits E2F1 transactivation domain binding to the pRb pocket domain. These vastly differing consequences of phosphorylation of pRb at different residues suggests that the effects of specific pRb phosphorylation events will have distinct impacts on cell fate.

One particular role for hyperphosphorylation of pRb that has come to light in recent years is its involvement in neurodegeneration. Several *in vitro* and *in vivo* studies have shown increased ppRb levels as evidence for aberrant cell cycle activation in various neurodegenerative processes. First, we have previously shown increased ppRb levels in neurons of patients afflicted with neurodegenerative disorders, including Alzheimer Disease (AD) and Parkinson Disease (PD) (Burke et al., 2010; Jordan-Sciutto et al., 2003; Jordan-Sciutto et al., 2002a), and in both HIV encephalitis (HIVE) (Jordan-Sciutto et al., 2002b), and a simian model of HIVE, SIVE (Jordan-Sciutto et al., 2000). *In vitro* studies have shown that forceful phosphorylation of pRb following cyclin D1 overexpression is sufficient to induce apoptosis of postmitotic neurons, further supporting a role for ppRb in disease (Freeman et al., 1994; Kranenburg et al., 1996). Additionally, other studies have demonstrated increased ppRb levels in post-mitotic neurons in response to trophic factor withdrawal, β-amyloid treatment, and oxidative stress (Giovanni et al., 1999; Liu and Greene, 2001; Padmanabhan et al., 1999), while inhibition of pRb phosphorylation by cyclin dependent kinases attenuated neuronal death induced by DNA damage and β-amyloid. However, we have also observed increased ppRb in murine neuronal cultures in response to the trophic factors, BDNF, NGF, and RANTES, with no apparent damage to the neurons (Strachan et al., 2005).

Given that several phosphorylation sites are known to have interactions with multiple proteins and considering that pRb function is dictated by its phosphorylation status, we reasoned that different stimuli may target discrete phosphorylation sites on pRb, leading to distinct outcomes in post-mitotic neurons, and might, therefore, explain the aforementioned contradictory observations regarding phosphorylation of pRb. In this study, we examined pRb phosphorylation patterns in primary mixed cortical cultures following treatment with trophic factors, Brain-derived neurotrophic factor (BDNF) and RANTES, or a neurotoxic factor, N-methyl D-aspartic acid (NMDA). Further, to determine whether any ppRb isotypes were specifically associated with HAND, we compared these phosphorylation patterns with those observed in cortical cultures in our *in vitro* model of HIV-induced neurodegeneration.

NIH-PA Author Manuscript

NIH-PA Author Manuscript

NIH-PA Author Manuscript

Our results show that HIV-MDM lead to an early increase in ppRb serine795 *in vitro*, as assessed by western blotting (WB) and immunofluorescence (IFA); whereas pRb was phosphorylated at serine608 and serine 807/811 residues in RANTES- and BDNF-treated cultures. Both trophic factor-induced and HIV-MDM-induced pRb phosphorylation were dependent on global CDK activation; however, only BDNF-induced pRb phosphorylation was dependent on the specific CDK, CDK5, which has known roles in both neuronal growth and neuronal death. Further, overexpression of a mutant pRb nonphosphorylatable at serine795 attenuated neuronal damage in our model of HIV-induced neurotoxicity. Finally, consistent with our *in vitro* findings, we observed a significant increase in ppRb serine795 by immunofluorescence and immunoblotting in the mid-frontal cortices of autopsied brain tissue of HIV(+) individuals. Collectively, these data support our hypothesis that pRb is differentially phosphorylated in neurons depending on the stimulus and, more specifically, that it is preferentially phosphorylated on serine795 in association with HIV infection in the CNS, suggesting that the prevailing phospho-pRb isoform affects the survival of post-mitotic neurons. Our findings also suggest that pRb may be an important target for intervention in prevention of neuronal damage in HAND.

2. Experimental Methods:

2.1 Chemicals and reagents:

N-methyl-D-aspartic acid (NMDA), Roscovitine, (+)-5-methyl-10,11-dihydro-5*H*-dibenzo[*a*,*d*]cyclohepten-5,10-imine maleate (MK801) and Olomoucine were from Tocris Bioscience (Ellisville, MO). Human recombinant BDNF was purchased from Promega (Madison, WI); mouse recombinant RANTES and Roscovitine were from Sigma-Aldrich (St. Louis, MO). Rabbit polyclonal antibody to ppRb threonine356 was from Novus Biologicals (Littleton, CO). Rabbit polyclonal antibodies to ppRb threonine249/S252 and ppRb threonine821 were purchased from Biosource Intl. Inc. (Camarillo, CA). Rabbit polyclonal antibodies to ppRb serine608, ppRb serine780, ppRb serine795 and ppRb serine807/S811 were from Cell Signaling (Danvers, MA). Mouse monoclonal antibody to MAP2 was purchased from Covance Research Products (Berkeley, CA, USA). Rabbit polyclonal antibody for GFAP was from Dako (Carpinteria, CA). The tyramide amplification system was purchased from New England Biolabs (Beverly, MA), and DAPI was from Molecular Probes (Carlsbad, CA).

2.2 Primary rat neuroglial cultures:

Primary rat neuroglial cultures were prepared from the cortex of embryonic day 17 Sprague Dawley rat pups, as described previously (Brewer, 1995). For western immunoblotting, cells were plated at a density of 2×10^6 cells per 60 mm dish pre-coated with poly-L-lysine (PLL) (Peptides International, Louisville, KY). For immunofluorescence studies, cells were plated on 10 mm PLL-coated glass coverslips at a density of 5×10^5 per coverslip. The cultures were maintained in neurobasal media (Invitrogen, Carlsbad, CA) with B27 supplement (Invitrogen) at 5% CO_2, 37°C. Half of the medium was replenished every seven days and cultures were utilized at 21 days *in vitro*.

2.3 Monocyte derived Macrophage (MDM) cultures:

Our *in vitro* model uses supernatants (HIV-MDM) from monocyte derived macrophages infected with a primary, macrophage tropic, HIV-1 isolate (Jago) collected from cell-free CSF of a patient with confirmed HAD, as described previously (Chen et al., 2002; O'Donnell et al., 2006; Wang et al., 2007). Briefly, primary blood mononuclear cells were isolated from healthy volunteers, as described previously (Chen et al., 2002), in accordance with protocols approved by the University of Pennsylvania Committee on Studies Involving Human Beings. Cells were differentiated for 7 days in macrophage media (DMEM with

NIH-PA Author Manuscript

NIH-PA Author Manuscript

NIH-PA Author Manuscript

10% fetal bovine serum, 10% horse serum, 1% penicillin/streptomycin, and 1% nonessential amino acids) in six-well plates (2.5×10^6 cells per well). On day 7, cultures were infected with cell-free HIV-1 inoculum (100 ng of p24 per well) and incubated for 24 h. Cells were washed twice with PBS and incubated in fresh macrophage media. HIV-MDM was monitored for up to 15-17 days for productive infection by p24 ELISA (NEN, Boston, MA). HIV infection of macrophages was confirmed by reverse transcriptase activity over time in each case, and only HIV-MDM supernatants exhibiting productive infection, as determined by reverse transcriptase activity, were used to treat neuronal cultures. HIV-MDM and mock-infected MDM (Mock) was collected at selected time points after infection and stored at −80°C. Cortical cultures were treated by addition of 1:20 dilution of supernatant directly to their culture media. As with other macrophage-tropic HIV strains, Jago productively infects primary T-lymphocytes and macrophages, but not transformed T-cell lines (Chen et al., 2002).

2.4 Construction of lentiviral vectors:

ppRbS795A and ppRbS795E plasmids were generated from pCMVNeoBam-pRbwt by site-directed mutagenesis using Quickchange XL mutagenesis kit (Stratagene, Santa Clara, CA) with the following primers: S795A forward (5′ CCTTACAAGTTTCCTAGTGCACCCTTACGGATTCCTG), S795A reverse (5′ CAGGAATCCGTAAGGGTGCACTAGGAAACTTGTAAGG) S795E forward (5′ CCTCGAAGCCCTTACAAGTTTCCTAGTGAGCCCTTACGGATTCC), S795E reverse (5′ GGAATCCGTAAGGGCTCACTAGGAAACTTGTAAGGGCTTCGAGG). The mutated plasmids, pCMVNeoBam-pRbS795A, pCMVNeoBam-pRbS795E and pCMVNeoBam-pRbwt, were cloned into the recombinant lentiviral cloning plasmid p1300 (University of Pennsylvania Vector Core) that contains GFP under the same promoter, using BamHI-BamHI restriction enzymes, and were packaged into recombinant lentiviral particles using the ViraPower lentiviral packaging kit (Invitrogen, CA). The number of viral particles generated were quantified using Lentivirus-Associated p24 ELISA Kit (Cell Biolabs, San Diego, CA). Ten viral particles per neuron were used for transduction studies.

2.5 Infection of primary neuroglial cultures with lentiviral vectors:

The media of 3-week-old primary rat neuroglial cultures in 60-mm dishes were changed one day prior to infection. The infections were carried out by addition of the thawed virus directly into the media of the culture at volumes not exceeding 10 μl. Experiments were carried out after three days of infection with lentiviral vectors.

2.6 Western immunoblotting for primary rat neuroglial cultures:

Whole cell extracts were lysed for 20 min with ice-cold lysis buffer consisting of 50 mM Tris pH 7.5, 120 mM NaCl, 0.5 % NP-40, 1mM PMFS, 20 U / ml aprotinin, 0.4 mM NaF, 5μg / ml leupeptin A and 0.4 mM Na_3VO_4. The lysates were centrifuged at 4°C for 15 min. The protein concentrations of supernatants were determined by the Bradford method (BioRad, Hercules, CA, USA). For each treatment, 50μg protein was used for western immunoblotting, as described previously. Primary rabbit polyclonal antibodies to ppRb threonine821, ppRb threonine356, ppRb serine608, ppRb serine780, ppRb serine795 or ppRb serine807/811, and HRP-conjugated secondary antibody (Pierce Biotechnology, Rockford) were used at a dilution of 1:1000. The membranes were developed using SuperSignal West Dura Extended Duration Substrate (Pierce Biotechnology, Rockford, IL). Loading controls were obtained by staining the PVDF membranes or the gels with the Coomassie Brilliant-Blue R-250 (BioRad) solution (0.1% Coomassie (w/v) in 50% Methanol) for 5 min, followed by destaining with 25% acetic acid in 50% methanol for 30 min. Densitometric band analysis was performed as described previously.

NIH-PA Author Manuscript

NIH-PA Author Manuscript

NIH-PA Author Manuscript

2.7 Quantification of neuronal damage and viability:

Primary rat neuroglial cultures were plated onto 96-well plates and maintained in neurobasal media supplemented with B27 for three weeks, followed by specified treatments. The plates were later assessed for MAP2 fluorescence using a MAP2 cell based ELISA, as described previously (White et al., 2011). In conjunction with this method, primary rat neuroglial cultures were also plated on coverslips and subjected to the same experimental conditions to determine neuronal viability by hand counting using propidium iodide (PI) exclusion. PI is taken up by dead cells, whereas live cells stain negative for the dye. 15 minutes before the end of the treatments, 15 μM PI was added to cultures. Following staining the cultures for MAP2, the coverslips were mounted on slides and alive/dead neurons were hand-counted based on loss of MAP2 and PI-positive staining.

2.8 Immunofluorescent confocal microscopy for primary rat neuroglial cultures:

Cells plated on coverslips were fixed in 4% paraformaldehyde for 30 minutes and washed 4 times in PBS, followed by blocking with 10% normal goat serum in PBS. Rabbit polyclonal antibodies to ppRb serine795, ppRb serine807/811 and GFAP, and mouse monoclonal antibody to MAP2 were used at empirically defined dilutions (ppRb serine795 at 1:5,000; MAP2 at 1:200; GFAP at 1:80). The tyramide amplification system (Lindl et al., 2007) was used to detect ppRb serine795 and ppRb serine807/811. ppRb serine795 and ppRb serine807/811 primary antibodies were detected by a biotin-conjugated, goat anti-rabbit secondary (1:600) antibody (Jackson ImmunoResearch Laboratories, Inc., West Grove, PA, USA) for use with the tyramide amplification system, and were subsequently visualized using FITC-conjugated streptavidin (New England Biolabs). The MAP2 and GFAP primary antibodies were visualized by a Cy-3-conjugated, goat anti-mouse antibody (1:200) and a Cy-5-conjugated goat anti-rabbit antibody (1:200), respectively. DNA was visualized by DAPI staining (5 μM). Slides were mounted in Citifluor AF1 (Citifluor, Ltd., London, UK) and were analyzed by laser confocal microscopy on a Biorad Radiance 2100 equipped with Argon, Green He/Ne, Red Diode, and Blue Diode lasers (Biorad), as described previously (Lindl et al., 2007). All images shown were captured with uniform threshold settings.

2.9 Human brain tissue:

Fresh frozen tissue samples from the midfrontal cortices of control (n=4) and HIV (+) (n=14) human autopsy cases used for this study were obtained from the tissue banks of National NeuroAIDS Tissue Consortium (NNTC) (Table 3). Whole cell lysates were obtained as described previously (Lindl et al., 2007). For western immunoblotting**,** 100 μg protein was loaded to each lane of 10 % Bis-Tris gels and processed further, as described above for primary rat neuroglial cultures.

2.10 Immunofluorescent confocal microscopy for human brain tissue:

Paraffin-embedded tissue sections from the cortices of control (n=4) and HIV (+) (n=14) human autopsy cases were obtained from the tissue banks of National NeuroAIDS Tissue Consortium (NNTC). Glass slides containing paraffin-embedded sections (7 μm) were de-paraffinized and re-hydrated, as described previously (Lindl et al., 2007). Endogenous peroxidase activity was inactivated by H_2O_2. Antigen unmasking was performed by placing slides in target retrieval solution (Dako, Carpinteria, CA, USA) at 95°C for 1h, and tissue sections were blocked with 10% normal goat serum in PBS. Rabbit polyclonal antibodies to ppRb serine795 and GFAP, and mouse monoclonal antibody to MAP2 were used at empirically defined dilutions (ppRb serine795 at 1:1,000; MAP2 at 1:100; GFAP at 1:80). The tyramide amplification system was used to detect ppRb serine795. Slides were mounted in Citifluor AF1 (Citifluor, Ltd., London, UK) and were analyzed by laser confocal microscopy, as described previously. All images shown were captured with uniform

NIH-PA Author Manuscript

NIH-PA Author Manuscript

NIH-PA Author Manuscript

threshold settings. Post-acquisition analysis for immunostaining was performed using MetaMorph 6.0 image analysis software (Universal Imaging, Inc, Downingtown, PA). Ten high-magnification (600X) images were captured randomly from the areas of positive staining in the mid-frontal cortical gray matter for each case. Nuclear ppRb serine795 was determined by the measurement of integrated pixel intensity for ppRb serine795 divided by the area where ppRb serine795 signal overlaps DAPI signal. The integrated pixel intensity is defined as total pixel intensity per image times the area of pixels positive for the signal. Averages are expressed at mean ± SEM. All data was analyzed by GraphPad Prism 3.02 software (GraphPad Software, San Diego, CA, USA).

2.11 Statistical Analysis:

One-way ANOVA with post-hoc Newman-Keuls multiple comparison test was used for statistical analysis of *in vitro* immunoblot quantification. For immunoblotting of human tissue samples, statistical analysis was performed between the post-mortem interval (PMI) and the relative ppRb serine795 levels, as detected by immunoblotting, to account for a possible correlation between these two parameters, and no correlation was found (r^2=0.1, p=0.2). For immunofluorescence and immunoblot studies of human tissue, student's t-test was performed. For all statistical analyses performed, values of $p < 0.05$ were considered significant.

3. Results

3.1 pRb is differentially phosphorylated in response to the neurotoxic HIV-MDM, as compared with phosphorylation induced by trophic factors, RANTES and BDNF.

Soluble neurotoxic factors, such as glutamate, quinolinic acid, and reactive oxygen species, as well as viral proteins released from HIV-infected monocyte-derived macrophages are proposed to be major determinants of neuronal death in HAND (Gendelman et al., 1994; Gonzalez-Scarano and Martin-Garcia, 2005b; Kaul et al., 2005). To recapitulate these conditions *in vitro*, we utilize a model in which we treat primary rat neuroglial cultures with supernatants (HIV-MDM) derived from monocyte-derived macrophages infected with a primary, macrophage tropic, HIV-1 isolate (Jago) collected from cell-free cerebrospinal fluid (CSF) of a patient with confirmed HAND. Importantly, we have previously demonstrated that HIV-MDM induces neuronal death via NMDA receptors in our *in vitro* model (O'Donnell et al., 2006; Wang et al., 2007). The supernatants from the peak of viral replication (days 9-12 post-infection) (Figure 1A) were used to treat 21 days *in vitro* (DIV) primary rat cortical cultures maintained in serum-free neural basal media. Neuronal damage in this model was assessed by a cell based ELISA, where loss of microtubule-associated protein2 (MAP2) reflects neuronal damage/death (Wang et al., 2007; White et al., 2011), which was further confirmed by propidium iodide exclusion via hand-counting of neurons (Figure 1B and C). As seen in Figure 1B, in cultures treated for 20 hours HIV-MDM supernatants from multiple different macrophage donors consistently lead to 65-80% neuronal death when diluted 20 times in culture media. Further, neurotoxicity achieved by HIV-MDM supernatants was dose-dependent (Figure 1C).

We had previously shown increased staining for phosphorylation of pRb at serine 795 in neurons in AD, PD, SIVE, and HIVE *in vivo* (Jordan-Sciutto et al., 2001; Jordan-Sciutto et al., 2003; Jordan-Sciutto et al., 2002a; Jordan-Sciutto et al., 2002b; Jordan-Sciutto et al., 2000). Further, we had also demonstrated that pRb is phosphorylated on serine795 in response to trophic factors, BDNF, NGF, and RANTES, in murine cortical cultures after 20 hours (Strachan et al., 2005). In the study presented here, we sought to examine which specific sites are phosphorylated in primary rat cortical, mixed neuroglial cultures exposed to HIV-MDM treatments, and, further, whether these sites or other sites are phosphorylated

NIH-PA Author Manuscript

NIH-PA Author Manuscript

NIH-PA Author Manuscript

in response to trophic factors or neurotoxic factors, given that pRb function is dictated by its phosphorylation status. Specifically, we examined pRb phosphorylation in response to the trophic factors, RANTES and BDNF, and to the neurotoxic factor, NMDA. There are nine commercially available antibodies for ppRb isoforms (Table 1) which recognize human and rat ppRb isoforms, enabling us to study phospho-sites in both the C and the N termini of pRb in both our model system and human tissue. Phosphorylation of pRb at each site was assessed after 1, 2, and 4 hours of treatment, as post-translational modifications of typical transcriptional regulators are expected to occur early. As shown in Figure 2A-C, serine608 and serine 807/811 are preferentially phosphorylated by RANTES and BDNF ($p<0.05$). On the other hand, of the six well-characterized phosphorylation sites we included in our studies, only serine795 was preferentially phosphorylated specifically by HIV-MDM but none of the other treatments within the studied time course (Figure 2A and 2D, $p<0.05$). To verify the pRb phospho-isoforms in HIV-MDM-treated neurons, we used a kinome assay (Kinexus). This independent approach confirmed phosphorylation at serine795 (data not shown). While HIV-MDM did target threonine249/252 and threonine821 (Figure 2A) for phosphorylation, mock-infected supernatants (Mock) also induced pRb phosphorylation at these sites, demonstrating that phosphorylation at these sites is not specific to treatment with supernatants from HIV-infected macrophages. The phospho-serine780 epitope of pRb, which was one of the first identified phosphorylation sites on pRb and is the most-widely used for pRb functionality in dividing cells, was not preferentially phosphorylated by either trophic factors or HIV-MDM (Figure 2E). Of note, none of the sites analyzed were phosphorylated by NMDA at the dose and time points we studied. However, we have previously shown that HIV-MDM induced NMDA receptor activation, contributing to neuronal death seen in this model (O'Donnell et al., 2006; Wang et al., 2007). While it could be argued that a component of the HIV-MDM acting through NMDA receptor will induce ppRb serine795 phosphorylation, we did not observe the abolishment of pRb phosphorylation at serine795 in HIV-MDM treated cultures pre-incubated with the NMDA receptor antagonist, MK801 (Figure 2F).

3.2 ppRb serine795 is increased in neuronal nuclei of primary rat cortical cultures in response to HIV-MDM, while ppRb serine807/serine811 is increased in neuronal cytoplasm in response to RANTES and BDNF.

pRb exerts its control over cell cycle primarily by binding to and inhibiting the activity of transcription factors and, thus, is expected to be localized to the nucleus. To determine the localization of phosphorylated pRb isoforms in neurons treated with trophic factors or neurotoxic factors, we utilized triple label immunofluorescent laser confocal microscopy. We observed increased ppRb serine795 immunoreactivity exclusively in the neuronal nuclei exposed to HIV-MDM (Figure 3, upper panel). On the contrary, serine807/serine811, a target for RANTES and BDNF, was detected predominantly in the cytoplasm of neurons (Figure 3, lower panel). Taken together, these findings suggest that pRb phosphorylation and the subcellular localization of ppRb in neurons is dependent on the stimuli *in vitro* (summarized in table 2).

3.3 Cyclin dependent kinase 5 (CDK5) preferentially phosphorylates pRb at serine608 and serine807/811 in response to BDNF.

Neurons express a unique cyclin dependent kinase, CDK5, for which the role in neuronal survival remains unclear. We have previously shown that, in neurons exposed to HIV-MDM, CDK5 contributes to death following calpain cleavage of its regulatory subunit, p35(Wang et al., 2007). Blocking CDK5 activity by a CDK5 inhibitor, Roscovitine, provides neuroprotection in our *in vitro* model of HIV-induced neurotoxicity (Wang et al., 2007). Interestingly, pRb is phosphorylated at serine807/811 by CDK5 in a neuroblastoma cell line, SH-SY5Y (Hamdane et al., 2005), a site which we have shown here to be targeted

NIH-PA Author Manuscript

NIH-PA Author Manuscript

NIH-PA Author Manuscript

by trophic factors, BDNF and RANTES. Further, BDNF has been shown to promote neuronal differentiation and survival through CDK5 activation (Cheung et al., 2007). To determine whether CDK5 targets pRb at serine795, which is in close vicinity of serine807/811 site, we examined pRb phosphorylation at this site in HIV-MDM- treated neurons, pre-incubated with Roscovitine. As shown in Figure 4A, we did not see a change in levels of ppRb serine795 in cultures pre-incubated with Roscovitine, as compared with those not pre-incubated with the CDK5 inhibitor when cells were exposed to HIV-MDM, suggesting that serine795 is not targeted by CDK5 for phosphorylation in our model. However, blocking all CDK activity by pan-CDK inhibitor, Olomoucine, effectively blocked HIV/MDM-induced formation of ppRb serine795 at 4 hours (Figure 4B), suggesting that a member of the CDK family other than CDK5 targets pRb at serine795. Of note, in cultures treated with HIV/MDM alone, ppRb serine795 did not increase at the 16 hour time-point in figure 4B, while it did increase at 16 hours in Figure 4A. This is most likely due to the slight variability at later time points in neurotoxicity induced by HIV/MDM produced in macrophages from different donors; the cultures used in figure 4B showed more neuronal death than those from Figure 4A (data not shown). On the other hand, CDK5 inhibition by Roscovitine abolished pRb phosphorylation at serine 608 and 807/811 in cultures exposed to BDNF (Figure 4C), suggesting that CDK5 acts as a kinase for pRb phosphorylation at these sites . Roscovitine and Olomoucine were not toxic at the concentration used in these studies (Figure 4D).

3.4 pRb serine795 phosphorylation contributes to HIV-MDM-induced neuronal death.

To determine whether serine795 phosphorylation is necessary for neuronal death in our *in vitro* model of HIV-associated neurodegeneration, we utilized a lentiviral expression system to overexpress a pRb mutant in which serine795 was mutated to either an alanine (ppRb S795A) or a glutamic acid (ppRb S795E) (Figure 5A). Alanine mutation renders the specific site nonphosphorylatable, whereas the glutamic acid mutation mimics a phosphorylated state. Neuronal viability as assayed by MAP2-cell based ELISA showed that 21 DIV neurons overexpressing ppRb S795A were less susceptible to HIV-MDM-induced toxicity as compared with neurons overexpressing wild-type pRb or ppRb S79E (Figure 5B, $p < 0.01$). These findings suggest that phosophorylation on pRb serine795 contributes to HIV-MDM-induced neuronal damage.

3.5 ppRb serine795 levels are increased in neuronal nuclei in mid-frontal cortices of HIV-infected individuals.

To determine whether the increase in ppRb serine795 expression we observed *in vitro* also occurs in HIV-infected human brain *in vivo*, we performed triple-label immunofluorescent laser confocal microscopy (TLCM) for ppRb serine795 and for phenotypic markers for astrocytes and neurons in the mid-frontal cortices of 14 HIV(+) and 4 HIV(−) control cases (summary of cases is included in table 3). This analysis allowed us to determine which cell types are expressing ppRb serine 795. We observed ppRb serine795 immunostaining predominantly in nuclei of neurons in gray matter (Figure 6A), whereas we did not detect ppRb serine795 in astrocytes in gray or white matter (data not shown). Further, quantitative analysis of the images obtained by TLCM showed that ppRb serine795 immunostaining was increased significantly in the HIV(+) group as compared with control cases (Figure 6B, * $p < 0.05$). Further, when the cases were grouped according to their neurocognitive status, there was a statistically significant increase in the ppRb serine795 immunostaining in the most severely compromised HAND cases (HAD-HAND) compared with the neurocognitively normal cases. Interestingly, ppRb serine795 increased in the less severely compromised group (non-HAD-HAND) compared with the HAD- HAND group (Figure 6C). Finally, we also examined ppRb serine807/811 expression in HIV-infected human brain via TLCM (not shown). We found that serine807/811 did not increase in HIV(+) cases compared with the

NIH-PA Author Manuscript

NIH-PA Author Manuscript

NIH-PA Author Manuscript

control group, as determined by quantification of TLCM images (quantification of images are shown in Figure 6D).

To further support our TCLM findings, we compared ppRb expression by immunoblotting in mid-frontal cortical tissue of the same cohort of cases used for TLCM. We observed increased expression of ppRb serine795 in the HIV(+) group as compared with the HIV(−) control cases (Figure 6E, 6F). The ppRb serine795 increase was significant in the neurocognitively impaired (HAND) group when compared with the neurocognitively normal group ($p < 0.05$, data not shown). Further, while it did not reach significance, ppRb serine795 expression showed a trend of increasing in the more severely cognitively compromised group (HAD-HAND) as compared with the less severely compromised group (non-HAD HAND) (Figure 6G), contrary to our observations using TLCM. As we had observed with TLCM, we did not detect a statistically significant change in ppRb serine 807/serine811 (Figure 6E, 6H). Further, we did not detect an increase in expression of other phosphorylated isoforms of pRb (threonine249/252, serine608, serine780, threonineT821; data not shown) by immunoblotting. Taken together, these data suggest that serine795 as a preferred site for phosphorylation in HIV-infected brain.

4. Discussion:

Regulators of cell cycle progression are common downstream targets of both the trophic and the neurotoxic factors implicated in HAND (Jordan-Sciutto et al., 2001; Jordan-Sciutto et al., 2003; Jordan-Sciutto et al., 2002a; Jordan-Sciutto et al., 2002b; Jordan-Sciutto et al., 2000; Ranganathan and Bowser, 2003). Increased phosphorylated pRb (ppRb) expression has been shown in various neurodegenerative diseases, such as AD, PD, and HIVE, supporting a role for pRb phosphorylation in cell cycle re-entry of neurons in disease. However, trophic factors, BDNF and RANTES, have also been shown to lead to an increase of ppRb in neurons in the absence of cell death *in vitro* (Strachan et al., 2005), suggesting alternative roles for pRb in neuronal survival.

In this study, we demonstrate that specific pRb phosphorylation at serine795 contributed to neuronal death in HIV-MDM-treated cortical neurons *in vitro*. We further show, by both immunostaining and immunoblot, an increase in ppRb serine795 levels *in vivo* in HIV-infected brain. ppRb serine795 is a known target for phosphorylation in response to mitogenic signals and has been shown to be phosphorylated in neurons of patients with AD and PD *in vivo*. Interestingly, in our *in vitro* model, as well as in HIVE *in vivo*, ppRb serine795 and its regulatory target, E2F1, both show an increase, but are detected in the nucleus and the cytoplasm (Wang et al., 2010), respectively, while hypophosphorylated pRb species can be detected in both cytoplasmic and nuclear fractions. Given that a previous study suggested that pRb serine795 phosphorylation causes pRb to dissociate from E2F1 (Rubin et al., 2005), loss of pRb:E2F1 interaction and nuclear translocation of ppRb serine795 could potentially be an underlying mechanism of neuronal death. Here we report that the overexpression of a pRb mutant that cannot be phosphorylated at serine795 (ppRb S795A) in neurons partially blocks neuronal damage caused by HIV-MDM, whereas the overexpression of a pRb mutant that mimics the phosphorylated form of pRb (ppRb S795E) does not accelerate neuronal damage or lead to neuronal death in the absence of stimulus. These results suggest that serine795 phosphorylation is necessary but not sufficient as a partial component of the neuronal death we observe in response to HIV-MDM. Perhaps another event, such as a concurrent or consecutive phosphorylation on pRb, as suggested before (Rubin et al., 2005), changes in E2F1 levels or other post-translational modifications of pRb needs to occur for the specific serine795 phosphorylation on pRb.

NIH-PA Author Manuscript

NIH-PA Author Manuscript

NIH-PA Author Manuscript

Interestingly, even though neuronal death in our *in vitro* model of HIV-induced neurotoxicity is mediated through activation of the NMDA glutamate receptor (O'Donnell et al., 2006; Wang et al., 2007), NMDA, which is an NMDA receptor agonist, did not induce phosphorylation of pRb on serine795 in cortical cultures at the time points and concentrations used in this study nor did an NMDA inhibitor, MK801, reduce levels of ppRb serine795 seen in these cultures. These findings suggest that an as yet undetermined mediator present in HIV-MDM acts as the trigger for pRb serine795 phosphorylation. Of note, while the toxicity observed in our model of HIV-associated neurodegeneration is entirely blocked by an NMDA receptor antagonist (O'Donnell et al., 2006), we show here that over-expression of a pRb mutant that is non-phosphorylatable at serine 795 also partially blocks death in our *in* vitro model. These data also suggest that ppRb serine795 exerts its influence on neuronal death through mechanisms that are downstream from NMDA receptor activity. Khan et al. (Khan et al., 2008) presented findings that support this conclusion when they showed that silencing of pRb partially reduced NMDA-induced toxicity in mixed rat cortical cultures. The exact composition of HIV-MDM cannot be identified with certainty; however, while it is expected to include trophic factors (Llano et al., 2003), such as BDNF and RANTES, in addition to neurotoxic factors, the extreme neurotoxicity of HIV-MDM suggests that the toxic factors in these supernatants play a stronger role in determining neuronal fate in this model. Thus it is not surprising that we observe increased pRb phosphorylation at serine795, which we show to contribute to the neurotoxicity in this model, rather than at serine608 or 807/811. In fact, it is possible that a toxic component of HIV-MDM is actually the blockage of pRb phosphorylation at sites that could induce a pro-survival function for pRb under normal conditions. Further studies with fractionated HIV-MDM are needed to dissect the pathways leading to specific pRb phosphorylation events and outline the specific mechanisms involved downstream from ppRb serine795.

Our current findings regarding pRb phosphorylation at serine795 in primary rat cortical cultures are in contrast to our previously published observations of increased ppRb serine795 levels in RANTES- and BDNF-treated primary mouse cultures *in vitro* (Strachan et al., 2005). There are several possibilities that could account for this discrepancy. First, the pRb phosphorylation profile might differ among species. Secondly, increased ppRb serine795 was observed at 24 hours after treatment of primary mouse cortical cultures with RANTES and BDNF, a much later time point compared with 1, 2, and 4 hours which we chose for our studies in primary rat cortical cultures. We chose earlier time points for this study as post-translational modifications of a transcriptional regulator such as pRb are expected to occur early in response to external stimuli. Our previous findings where ppRb serine795 was induced by BDNF or RANTES in mouse neurons (Strachan et al., 2005) could be a result of more than one primary pathway triggered by the specific factors studied, as the end-point of those treatments were 24 hours. Finally and most importantly, the ages of cultures used in these two studies are different. While we previously used mouse cortical cultures after 7 days *in vitro* (Strachan et al., 2005), this study utilized 3-week-old rat cortical cultures. As a cell-cycle related protein, the cellular functions of pRb, and thus the specific phosphorylation patterns, would be expected to be dependent on the age of the culture, especially since neurons undergo cell-cycle exit as they differentiate. In this study, we chose 3-week-old cultures for our studies for several reasons. First, as we have shown previously, primary rat cultures become susceptible to HIV-MDM-induced damage only after 2½ weeks *in vitro* (O'Donnell et al., 2006; Wang et al., 2007), when they express either monomeric NMDA 2A/2A or heteromeric NMDA2A/2B subunits that render neurons susceptible to HIV-MDM-induced neurotoxicity. Secondly, we used 3-week-old cultures, when they would be expected to be more differentiated, and would better reflect *in vivo* events affecting post-mitotic neurons in our *in vitro* model.

NIH-PA Author Manuscript

NIH-PA Author Manuscript

NIH-PA Author Manuscript

CDK5 appears to serve dual functions in the CNS, with roles in both disease and development. CDK5 activation has been detected in a wide variety of neurodegenerative disorders (Chergui et al., 2004; Henchcliffe and Burke, 1997; Nguyen et al., 2001; Pei et al., 1998a, b; Tseng et al., 2002; Zheng et al., 2005). Indeed, we have previously shown that excitotoxic amino acids present in supernatants of monocyte-derived macrophages infected with HIV lead to NMDA receptor-mediated neuronal death *in vitro* (Wang et al., 2007). In our model, NMDA receptor activation and the consequent influx of calcium results in activation of calcium-dependent, cysteine proteases called calpains. Calpain activation then causes increased CDK5 kinase activity and ultimately results in neuronal death. While the exact mechanism by which increased CDK5 kinase activity leads to neuronal death is not clear, it is plausible that CDK5, a member of the cyclin dependent kinase family, might regulate phosphorylation of pRb at serine795. However, the CDK5 inhibitor, Roscovitine, did not prevent the increased ppRb serine795 levels that we observed in cortical cultures in response to HIV-MDM, whereas global CDK inhibition by Olomoucine did block this ppRb serine795 formation. These data suggest that CDK5 does not act as a kinase for ppRb serine795 formation in our *in vitro* model of HIV-associated neurodegeneration, but rather a different CDK induces phosphorylation of pRb at serine795. Future studies using specific CDK inhibitors are needed to specifically identify the kinase responsible for ppRb serine795 generation in our *in vitro* model.

The second main role CDK5 plays in the CNS is during neuronal development. Mainly, CDK5 is required for proper cortical lamination and for regulation of diverse neuronal functions including neurite outgrowth and axonal migration (Dhavan and Tsai, 2001). One report suggests that c-abl-mediated CDK5 phosphorylation and subsequent increase in CDK5/p35 kinase activity plays a role in neurite outgrowth (Zukerberg et al., 2000). Serine807/811 is identified as a binding site for c-abl (Knudsen and Wang, 1996), a non-receptor tyrosine kinase which binds to the tyrosine kinase receptor A (trkA) neurotrophin receptor (Yano et al., 2000). c-abl regulates neurogenesis, neurite outgrowth, and plasticity, partially through its association with the actin cytoskeleton; however, trkA is only present in very low levels in the CNS (Harbott and Nobes, 2005; Jones et al., 2004; Maness, 1992; Woodring et al., 2002). Interestingly, it is through binding to trkB that BDNF has been shown to contribute to neuroprotection and neurite growth (Barnabe-Heider and Miller, 2003; Benoit et al., 2001; Fukumitsu et al., 2006; Takahashi et al., 1999). While no report shows c-abl binding to trkB, it is conceivable that an association might occur between the BDNF receptor, trkB, and c-abl, at least in neurons. Additionally, in dividing or postmitotic cells, not much data exists for the exact role of serine608, a site at which we also observed increased phosphorylation in our cortical cultures treated with BDNF and RANTES. Thus, our data implicating CDK5 as a kinase involved in the formation of ppRb serine807/811 and ppRb serine608 in BDNF-treated cultures further suggest that these isoforms indeed play a role in neuronal differentiation, neurite outgrowth, and survival. Interestingly, our previous observation that CDK5 is activated in response to treatment with HIV-MDM (Wang et al., 2007), yet we do not observe increased ppRb807/811 or ppRb608 in these HIV-MDM-treated cultures. This suggests that phosphorylation at these pRb residues may be actively blocked in our *in vitro* model, possibly contributing to the toxicity of HIV-MDM, as we mention above.

We have previously reported that the transcription factor E2F1, whose transactivation is classically identified to be dependent on pRb phosphorylation, is predominantly localized to the postmitotic neuronal cytoplasm (Jordan-Sciutto et al., 2002b), and in our *in vitro* model of HIV, as well as in HAND cortex *in vivo*, its classical transcriptional targets are not activated despite an increased cytoplasmic E2F1 expression (Wang et al., 2010). As we have stated previously, Chk1/2 has been shown to phosphorylate pRb at serine608, mounting a DNA damage response by facilitating pRb:E2F1 formation (Inoue et al., 2007). Given our

NIH-PA Author Manuscript

NIH-PA Author Manuscript

NIH-PA Author Manuscript

observation that pRb is phosphorylated at serine608 in response to trophic factors whereas preferential phosphorylation of pRb at serine795 occurs in disease state, nuclear ppRbS795 might very well preclude pRb:E2F1 complex formation in the cytoplasm in HAND where both trophic and neurotoxic factors are present, and contribute to the fate of the neuron. Studies utilizing pRb mutants nonphosphorylatable at serine608 will more clearly define the roles cytoplasmic phospho-pRb might play in neuronal survival in conjunction with E2F1.

Finally, our *in vivo* data also suggest pRb phosphorylation at serine795 as a unique site in HAND. ppRb serine795 was increased in HIV(−) cases were compared with the HIV(+) cases as detected by both immunofluorescence (IFA) and immunoblotting (IB). Further, when the cases were stratified according to their neurocognitive status, the HAD group show significantly greater ppRb serine795 staining than the neurocognitively normal group, which included both HIV(−) cases and HIV(+) cases with no neurocognitive impairments. Further, by IB, ppRb serine795 showed a trend of increasing in the HAD group, as compared with less the severely neurocognitively compromised group (non-HAD HAND). However, by IFA the opposite trend was observed. The main caveat of analyzing human samples is the variability across samples, which is going to be particularly apparent across tissue prepared for different methodologies, such as IFA and IB, as the areas processed vary between the methods. Unfortunately, this is especially important in HAND, as it is a focal disease even within the brain regions that are affected more frequently. One way to partially alleviate this is to expand these studies to a bigger cohort of cases. Another caveat in the case of IB is that the protein lysates by nature contain cellular proteins from glial cells and macrophage/microglia in addition to neurons. Thus, the changes in the levels any specific protein examined will be reflective of changes of that protein in multiple cell types, which can complicate analysis and interpretation. Since, as can be seen by IFA, ppRb serine795 is predominantly neuronal, varying ratios of different cell types in the lysates prepared for IB will certainly complicate analysis of IB data for this particular protein. Thus, analysis of changes in targets should be achieved by multiple methods where human samples are concerned. We show that ppRb serine795 is increased in the HIV (+) cases by two complementary methods, IFA and IB, an approach that partially compensates for the inherent variability observed in human samples.

In summary, our current findings suggest that pRb plays a multi-faceted role in neuronal survival in postmitotic neurons. Further, the functionality of pRb is determined by the phosphorylation state of specific pRb residues. While serine807/serine811 and serine608 are targeted for phosphorylation by trophic factors, serine795 appears to be a unique site in HAND both *in vitro* and *in vivo.* Finally, CDK5 appears to preferentially phosphorylate ppRb serine608 and serine807/811, suggesting that these ppRb isoforms may play a role in neuronal maintenance and neurite outgrowth in postmitotic neurons. Taken together, these findings suggest that HIV-infection in the brain is associated with site-specific hyperphosphoylation of pRb at serine795, which contributes to neuronal death in this disease. Our findings further demonstrate that specific pRb sites are differentially targeted and may serve as a unique target for therapeutic intervention for neurodegenerative diseases with a prominent neuroinflammatory component, such as HAND.

Acknowledgments

We would like to thank Dr. Marc A. Dichter and Margaret A. Maronski for providing us with primary cultures. We also thank National NeuroAIDS Tissue Consortium (NNTC) (supported by NIMH and NINDS, contract NIH-N01MH32002) for providing us with human tissue samples, and University of Pennsylvania Vector Core for the lentiviral plasmid. Finally, we thank the members of the Kolson, Gonzalez-Scarano, and Jordan-Sciutto laboratories for critical evaluation of our work.

NIH-PA Author Manuscript

NIH-PA Author Manuscript

NIH-PA Author Manuscript

Grants: This work was supported by the following grants: NS41202 (KJS), NS043994 (DLK), and T32AI-07632-06 (MGW).

References:

Achim CL, Masliah E, Heyes MP, Sarnacki P, Hilty C, Baldwin M, Wiley CA. Macrophage Activation Factors
in the Brains of AIDS Patients. Journal of neuro-AIDS. 1996; 1:1–16. [PubMed: 16873161]

Barnabe-Heider F, Miller FD. Endogenously produced neurotrophins regulate survival and differentiation of cortical progenitors via distinct signaling pathways. J Neurosci. 2003; 23:5149–5160. [PubMed: 12832539]

Benoit BO, Savarese T, Joly M, Engstrom CM, Pang L, Reilly J, Recht LD, Ross AH, Quesenberry PJ. Neurotrophin channeling of neural progenitor cell differentiation. Journal of neurobiology. 2001; 46:265–280. [PubMed: 11180154]

Brewer GJ. Serum-free B27/neurobasal medium supports differentiated growth of neurons from the striatum, substantia nigra, septum, cerebral cortex, cerebellum, and dentate gyrus. J Neurosci Res. 1995; 42:674–683. [PubMed: 8600300]

Burke JR, Deshong AJ, Pelton JG, Rubin SM. Phosphorylation-induced conformational changes in the retinoblastoma protein inhibit E2F transactivation domain binding. The Journal of biological chemistry. 2010; 285:16286–16293. [PubMed: 20223825]

Chen W, Sulcove J, Frank I, Jaffer S, Ozdener H, Kolson DL. Development of a human neuronal cell model for human immunodeficiency virus (HIV)-infected macrophage-induced neurotoxicity: apoptosis induced by HIV type 1 primary isolates and evidence for involvement of the Bcl-2/Bcl-xL-sensitive intrinsic apoptosis pathway. Journal of virology. 2002; 76:9407–9419. [PubMed: 12186923]

Chergui K, Svenningsson P, Greengard P. Cyclin-dependent kinase 5 regulates dopaminergic and glutamatergic transmission in the striatum. Proc Natl Acad Sci U S A. 2004; 101:2191–2196. [PubMed: 14769920]

Cheung ZH, Chin WH, Chen Y, Ng YP, Ip NY. Cdk5 is involved in BDNF-stimulated dendritic growth in hippocampal neurons. PLoS biology. 2007; 5:e63. [PubMed: 17341134]

Conant K, Garzino-Demo A, Nath A, McArthur JC, Halliday W, Power C, Gallo RC, Major EO. Induction of monocyte chemoattractant protein-1 in HIV-1 Tat-stimulated astrocytes and elevation in AIDS dementia. Proc Natl Acad Sci U S A. 1998; 95:3117–3121. [PubMed: 9501225]

Connell-Crowley L, Harper JW, Goodrich DW. Cyclin D1/Cdk4 regulates retinoblastoma protein-mediated cell cycle arrest by site-specific phosphorylation. Molecular biology of the cell. 1997; 8:287–301. [PubMed: 9190208]

DeGregori J, Leone G, Miron A, Jakoi L, Nevins J. Distinct roles for E2F proteins in cell growth control and apoptosis. Proc. Natl. Acad. Sci. USA. 1997; 94:7245–7250. [PubMed: 9207076]

Dhavan R, Tsai LH. A decade of CDK5. Nat Rev Mol Cell Biol. 2001; 2:749–759. [PubMed: 11584302]

Dore GJ, Correll PK, Li Y, Kaldor JM, Cooper DA, Brew BJ. Changes to AIDS dementia complex in the era of highly active antiretroviral therapy. AIDS (London, England). 1999; 13:1249–1253.

Everall IP, Trillo-Pazos G, Bell C, Mallory M, Sanders V, Masliah E. Amelioration of neurotoxic effects of HIV envelope protein gp120 by fibroblast growth factor: a strategy for neuroprotection. J Neuropathol Exp Neurol. 2001; 60:293–301. [PubMed: 11245213]

Freeman R, Estus S, Johnson E Jr. Analysis of cell cycle-related gene expression in postmitotic neurons: selective induction of cyclin D1 during programmed cell death. Neuron. 1994; 12:343–355. [PubMed: 8110463]

Frolov MV, Dyson NJ. Molecular mechanisms of E2F-dependent activation and pRB-mediated repression. Journal of cell science. 2004; 117:2173–2181. [PubMed: 15126619]

Fukumitsu H, Ohtsuka M, Murai R, Nakamura H, Itoh K, Furukawa S. Brain-derived neurotrophic factor participates in determination of neuronal laminar fate in the developing mouse cerebral cortex. J Neurosci. 2006; 26:13218–13230. [PubMed: 17182772]

NIH-PA Author Manuscript

NIH-PA Author Manuscript

NIH-PA Author Manuscript

Galicia O, Sanchez-Alavez M, Mendez Diaz M, Navarro L, Prospero-Garcia O. [HIV glycoprotein 120: possible etiological agent of AIDS-associated dementia]. Revista de investigacion clinica; organo del Hospital de Enfermedades de la Nutricion. 2002; 54:437–452.

Gendelman HE, Lipton SA, Tardieu M, Bukrinsky MI, Nottet HS. The neuropathogenesis of HIV-1 infection. 1994 [see comment]. [Review] [107 refs].

Giovanni A, Wirtz-Bruger F, Keramaris E, Slack R, Park D. Involvement of cell cycle elements, cyclin-dependent kinases, pRb, and E2F-DP, in B-amyloid-induced neuronal death. J. Biol. Chem. 1999; 274:19011–19016. [PubMed: 10383401]

Gisolf EH, van Praag RM, Jurriaans S, Portegies P, Goudsmit J, Danner SA, Lange JM, Prins JM. Increasing cerebrospinal fluid chemokine concentrations despite undetectable cerebrospinal fluid HIV RNA in HIV-1-infected patients receiving antiretroviral therapy. Journal of acquired immune deficiency syndromes. 2000; 25:426–433. 1999. [PubMed: 11141242]

Giulian D, Yu J, Li X, Tom D, Li J, Wendt E, Lin SN, Schwarcz R, Noonan C. Study of receptor-mediated neurotoxins released by HIV-1-infected mononuclear phagocytes found in human brain. J Neurosci. 1996; 16:3139–3153. [PubMed: 8627353]

Gonzalez-Scarano F, Martin-Garcia J. The neuropathogenesis of AIDS. Nature reviews. 2005a; 5:69–81.

Gonzalez-Scarano F, Martin-Garcia J. The neuropathogenesis of AIDS. 2005b [Review] [173 refs].

Hallstrom TC, Nevins JR. Specificity in the activation and control of transcription factor E2F-dependent apoptosis. Proceedings of the National Academy of Sciences of the United States of America. 2003; 100:10848–10853. [PubMed: 12954980]

Hamdane M, Bretteville A, Sambo AV, Schindowski K, Begard S, Delacourte A, Bertrand P, Buee L. p25/Cdk5-mediated retinoblastoma phosphorylation is an early event in neuronal cell death. Journal of cell science. 2005; 118:1291–1298. [PubMed: 15741232]

Hamel PA, Cohen BL, Sorce LM, Gallie BL, Phillips RA. Hyperphosphorylation of the retinoblastoma gene product is determined by domains outside the simian virus 40 large-T-antigen-binding regions. Mol Cell Biol. 1990; 10:6586–6595. [PubMed: 2174110]

Harbott LK, Nobes CD. A key role for Abl family kinases in EphA receptor-mediated growth cone collapse. Molecular and cellular neurosciences. 2005; 30:1–11. [PubMed: 15996481]

Harbour JW, Dean DC. Rb function in cell-cycle regulation and apoptosis. Nature cell biology. 2000a; 2:E65–67.

Harbour JW, Dean DC. The Rb/E2F pathway: expanding roles and emerging paradigms. Genes Dev. 2000b; 14:2393–2409. [PubMed: 11018009]

Heaton RK, Clifford DB, Franklin DR Jr. Woods SP, Ake C, Vaida F, Ellis RJ, Letendre SL, Marcotte TD, Atkinson JH, Rivera-Mindt M, Vigil OR, Taylor MJ, Collier AC, Marra CM, Gelman BB, McArthur JC, Morgello S, Simpson DM, McCutchan JA, Abramson I, Gamst A, Fennema-Notestine C, Jernigan TL, Wong J, Grant I. HIV-associated neurocognitive disorders persist in the era of potent antiretroviral therapy: CHARTER Study. Neurology. 2010; 75:2087–2096. [PubMed: 21135382]

Henchcliffe C, Burke RE. Increased expression of cyclin-dependent kinase 5 in induced apoptotic neuron death in rat substantia nigra. Neuroscience letters. 1997; 230:41–44. [PubMed: 9259459]

Inoue Y, Kitagawa M, Taya Y. Phosphorylation of pRB at Ser612 by Chk1/2 leads to a complex between pRB and E2F-1 after DNA damage. The EMBO journal. 2007; 26:2083–2093. [PubMed: 17380128]

Jones SB, Lu HY, Lu Q. Abl tyrosine kinase promotes dendrogenesis by inducing actin cytoskeletal rearrangements in cooperation with Rho family small GTPases in hippocampal neurons. J Neurosci. 2004; 24:8510–8521. [PubMed: 15456825]

Jordan-Sciutto K, Rhodes J, Bowser R. Altered subcellular distribution of transcriptional regulators in response to Abeta peptide and during Alzheimer's disease. Mechanisms of Ageing & Development. 2001; 123:11–20. [PubMed: 11640947]

Jordan-Sciutto KL, Dorsey R, Chalovich EM, Hammond RR, Achim CL. Expression patterns of retinoblastoma protein in Parkinson disease. Journal of Neuropathology & Experimental Neurology. 2003; 62:68–74. [PubMed: 12528819]

NIH-PA Author Manuscript

NIH-PA Author Manuscript

NIH-PA Author Manuscript

Jordan-Sciutto KL, Malaiyandi LM, Bowser R. Altered distribution of cell cycle transcriptional regulators during Alzheimer disease. Journal of Neuropathology & Experimental Neurology. 2002a; 61:358–367. [PubMed: 11939591]

Jordan-Sciutto KL, Wang G, Murphey-Corb M, Wiley CA. Cell cycle proteins exhibit altered expression patterns in lentiviral-associated encephalitis. Journal of Neuroscience. 2002b; 22:2185–2195. [PubMed: 11896158]

Jordan-Sciutto KL, Wang G, Murphy-Corb M, Wiley CA. Induction of cell-cycle regulators in simian immunodeficiency virus encephalitis. American Journal of Pathology. 2000; 157:497–507. [PubMed: 10934153]

Kaul M, Zheng J, Okamoto S, Gendelman HE, Lipton SA. HIV-1 infection and AIDS: consequences for the central nervous system. 2005 [Review] [199 refs].

Khan MZ, Brandimarti R, Shimizu S, Nicolai J, Crowe E, Meucci O. The chemokine CXCL12 promotes survival of postmitotic neurons by regulating Rb protein. Cell death and differentiation. 2008; 15:1663–1672. [PubMed: 18583990]

Kitagawa M, Higashi H, Jung HK, Suzuki-Takahashi I, Ikeda M, Tamai K, Kato J, Segawa K, Yoshida E, Nishimura S, Taya Y. The consensus motif for phosphorylation by cyclin D1-Cdk4 is different from that for phosphorylation by cyclin A/E-Cdk2. The EMBO journal. 1996; 15:7060–7069. [PubMed: 9003781]

Knudsen ES, Wang JY. Differential regulation of retinoblastoma protein function by specific Cdk phosphorylation sites. Journal of Biological Chemistry. 1996; 271:8313–8320. [PubMed: 8626527]

Knudsen ES, Wang JY. Dual mechanisms for the inhibition of E2F binding to RB by cyclin-dependent kinase-mediated RB phosphorylation. Mol Cell Biol. 1997; 17:5771–5783. [PubMed: 9315635]

Kranenburg O, van der Eb AJ, Zantema A. Cyclin D1 is an essential mediator of apoptotic neuronal cell death. The EMBO journal. 1996; 15:46–54. [PubMed: 8598205]

Lees JA, Buchkovich KJ, Marshak DR, Anderson CW, Harlow E. The retinoblastoma protein is phosphorylated on multiple sites by human cdc2. The EMBO journal. 1991; 10:4279–4290. [PubMed: 1756735]

Lin BT, Gruenwald S, Morla AO, Lee WH, Wang JY. Retinoblastoma cancer suppressor gene product is a substrate of the cell cycle regulator cdc2 kinase. The EMBO journal. 1991; 10:857–864. [PubMed: 2009861]

Lindl KA, Akay C, Wang Y, White MG, Jordan-Sciutto KL. Expression of the endoplasmic reticulum stress response marker, BiP, in the central nervous system of HIV-positive individuals. Neuropathol Appl Neurobiol. 2007; 33:658–669. [PubMed: 17931354]

Liu DX, Greene LA. Neuronal apoptosis at the G1/S cell cycle checkpoint. Cell & Tissue Research. 2001; 305:217–228. [PubMed: 11545259]

Llano A, Barretina J, Gutierrez A, Clotet B, Este JA. Interleukin-7-Dependent Production of RANTES That Correlates with Human Immunodeficiency Virus Disease Progression. J. Virol. 2003; 77:4389–4395. [PubMed: 12634395]

Maness PF. Nonreceptor protein tyrosine kinases associated with neuronal development. Developmental neuroscience. 1992; 14:257–270. [PubMed: 1295748]

Masliah E, DeTeresa RM, Mallory ME, Hansen LA. Changes in pathological findings at autopsy in AIDS cases for the last 15 years. AIDS (London, England). 2000; 14:69–74.

McArthur JC. HIV dementia: an evolving disease. Journal of neuroimmunology. 2004; 157:3–10. [PubMed: 15579274]

Navia BA, Cho ES, Petito CK, Price RW. The AIDS dementia complex: II. Neuropathology. Annals of Neurology. 1986; 19:525–535. [PubMed: 3014994]

Neuenburg JK, Brodt HR, Herndier BG, Bickel M, Bacchetti P, Price RW, Grant RM, Schlote W. HIV-related neuropathology, 1985 to 1999: rising prevalence of HIV encephalopathy in the era of highly active antiretroviral therapy. Journal of acquired immune deficiency syndromes. 2002; 31:171–177. 1999. [PubMed: 12394795]

Nguyen MD, Lariviere RC, Julien JP. Deregulation of Cdk5 in a mouse model of ALS: toxicity alleviated by perikaryal neurofilament inclusions. Neuron. 2001; 30:135–147. [PubMed: 11343650]

NIH-PA Author Manuscript

NIH-PA Author Manuscript

NIH-PA Author Manuscript

Nuovo GJ, Alfieri ML. AIDS dementia is associated with massive, activated HIV-1 infection and concomitant expression of several cytokines. Molecular Medicine. 1996; 2:358–366. [PubMed: 8784788]

O'Donnell LA, Agrawal A, Jordan-Sciutto KL, Dichter MA, Lynch DR, Kolson DL. Human immunodeficiency virus (HIV)-induced neurotoxicity: roles for the NMDA receptor subtypes. Journal Of Neuroscience. 2006

Padmanabhan J, Park DS, Greene LA, Shelanski ML. Role of cell cycle regulatory proteins in cerebellar granule neuron apoptosis. J Neurosci. 1999; 19:8747–8756. [PubMed: 10516294]

Pei JJ, Grundke-Iqbal I, Iqbal K, Bogdanovic N, Winblad B, Cowburn RF. Accumulation of cyclin-dependent kinase 5 (cdk5) in neurons with early stages of Alzheimer's disease neurofibrillary degeneration. Brain Research. 1998a; 797:267–277. [PubMed: 9666145]

Pei JJ, Grundke-Iqbal I, Iqbal K, Bogdanovic N, Winblad B, Cowburn RF. Accumulation of cyclin-dependent kinase 5 (cdk5) in neurons with early stages of Alzheimer's disease neurofibrillary degeneration. Brain research. 1998b; 797:267–277. [PubMed: 9666145]

Portegies P, Enting RH, deGans J, Algra PR, Derix MM, Lange JM, Goudsmit J. Presentation and course of AIDS dementia complex: 10 years of follow-up in Amsterdam, The Netherlands. AIDS (London, England). 1993; 7:669–675.

Power C, Johnson RT. HIV-1 associated dementia: clinical features and pathogenesis. The Canadian journal of neurological sciences. 1995; 22:92–100. [PubMed: 7627922]

Price RW, Brew B, Sidtis J, Rosenblum M, Scheck AC, Cleary P. The brain in AIDS: central nervous system HIV-1 infection and AIDS dementia complex. Science. 1988; 239:586–592. [PubMed: 3277272]

Ranganathan S, Bowser R. Alterations in G(1) to S phase cell-cycle regulators during amyotrophic lateral sclerosis. American Journal of Pathology. 2003; 162:823–835. [PubMed: 12598317]

Rubin SM, Gall AL, Zheng N, Pavletich NP. Structure of the Rb C-terminal domain bound to E2F1-DP1: a mechanism for phosphorylation-induced E2F release. Cell. 2005; 123:1093–1106. [PubMed: 16360038]

Sippy BD, Hofman FM, Wallach D, Hinton DR. Increased expression of tumor necrosis factor-alpha receptors in the brains of patients with AIDS. J Acquir Immune Defic Syndr Hum Retrovirol. 1995; 10:511–521. [PubMed: 8548330]

Soontornniyomkij V, Wang G, Pittman CA, Wiley CA, Achim CL. Expression of brain-derived neurotrophic factor protein in activated microglia of human immunodeficiency virus type 1 encephalitis. Neuropathology and applied neurobiology. 1998; 24:453–460. [PubMed: 9888155]

Strachan GD, Kopp AS, Koike MA, Morgan KL, Jordan-Sciutto KL. Chemokine- and neurotrophic factor-induced changes in E2F1 localization and phosphorylation of the retinoblastoma susceptibility gene product (pRb) occur by distinct mechanisms in murine cortical cultures. 2005

Takahashi J, Palmer TD, Gage FH. Retinoic acid and neurotrophins collaborate to regulate neurogenesis in adult-derived neural stem cell cultures. Journal of neurobiology. 1999; 38:65–81. [PubMed: 10027563]

Tseng HC, Zhou Y, Shen Y, Tsai LH. A survey of Cdk5 activator p35 and p25 levels in Alzheimer's disease brains. FEBS letters. 2002; 523:58–62. [PubMed: 12123804]

Ullrich CK, Groopman JE, Ganju RK. HIV-1 gp120- and gp160-induced apoptosis in cultured endothelial cells is mediated by caspases. Blood. 2000; 96:1438–1442. [PubMed: 10942389]

Wang Y, Shyam N, Ting JH, Akay C, Lindl KA, Jordan-Sciutto KL. E2F1 localizes predominantly to neuronal cytoplasm and fails to induce expression of its transcriptional targets in human immunodeficiency virus-induced neuronal damage. Neuroscience letters. 2010; 479:97–101. [PubMed: 20580656]

Wang Y, White MG, Akay C, Chodroff RA, Robinson J, Lindl KA, Dichter MA, Qian Y, Mao Z, Kolson DL, Jordan-Sciutto KL. Activation of cyclin-dependent kinase 5 by calpains contributes to human immunodeficiency virus-induced neurotoxicity. J Neurochem. 2007; 103:439–455. [PubMed: 17897354]

White MG, Wang Y, Akay C, Lindl KA, Kolson DL, Jordan-Sciutto KL. Parallel high throughput neuronal toxicity assays demonstrate uncoupling between loss of mitochondrial membrane

NIH-PA Author Manuscript

NIH-PA Author Manuscript

NIH-PA Author Manuscript

potential and neuronal damage in a model of HIV-induced neurodegeneration. Neuroscience research. 2011

Woodring PJ, Litwack ED, O'Leary DD, Lucero GR, Wang JY, Hunter T. Modulation of the F-actin cytoskeleton by c-Abl tyrosine kinase in cell spreading and neurite extension. The Journal of cell biology. 2002; 156:879–892. [PubMed: 11864995]

Woods S, Moore D, Weber E, Grant I. Cognitive Neuropsychology of HIV-Associated Neurocognitive Disorders. Neuropsychology Review. 2009; 19:152–168. [PubMed: 19462243]

Yano H, Cong F, Birge RB, Goff SP, Chao MV. Association of the Abl tyrosine kinase with the Trk nerve growth factor receptor. Journal of neuroscience research. 2000; 59:356–364. [PubMed: 10679771]

Zarkowska T, Mittnacht S. Differential phosphorylation of the retinoblastoma protein by G1/S cyclin-dependent kinases. The Journal of biological chemistry. 1997; 272:12738–12746. [PubMed: 9139732]

Zheng YL, Kesavapany S, Gravell M, Hamilton RS, Schubert M, Amin N, Albers W, Grant P, Pant HC. A Cdk5 inhibitory peptide reduces tau hyperphosphorylation and apoptosis in neurons. The EMBO journal. 2005; 24:209–220. [PubMed: 15592431]

Zukerberg LR, Patrick GN, Nikolic M, Humbert S, Wu CL, Lanier LM, Gertler FB, Vidal M, Van Etten RA, Tsai LH. Cables links Cdk5 and c-Abl and facilitates Cdk5 tyrosine phosphorylation, kinase upregulation, and neurite outgrowth. Neuron. 2000; 26:633–646. [PubMed: 10896159]

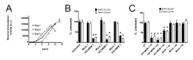

Figure 1. HIV-infected monocyte-derived macrophage supernatants cause neuronal death *in vitro*.

A) Reverse transcriptase activity of supernatants collected from HIV-infected human monocyte-derived macrophages (HIV-MDM) from three donors used in this study is shown. **B)** Loss of MAP2 as measured by MAP2 cell-based ELISA (black bars) and PI exclusion assay via hand counting (gray bars) of primary rat cortical cultures 21 DIV treated for 20 hours with HIV-MDM from three donors at a dilution of 1:20, as compared with untreated cultures or mock-infected MDM supernatants. **C)** Mock or HIV-MDM were diluted into the media of primary rat cortical neuroglial cultures 21 DIV for 20 hours and neuronal viability was measured by MAP2 ELISA (black bars) and PI exclusion assay (gray bars). (Student's t-test, * $p < 0.01$)

NIH-PA Author Manuscript
NIH-PA Author Manuscript
NIH-PA Author Manuscript

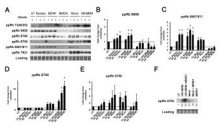

Figure 2. Site-specific phosphorylation of pRb phosphorylation is dependent on the stimulus.

A) Western immunoblotting of one set of extracts for expression of the six phospho-pRb forms included in this study is shown. HIV-MDM treatment resulted in phosphorylation of pRb at serine795, while RANTES and BDNF lead to increased pRb phosphorylation on serine608 and serine807/811. Fold changes of ppRb serine608 **(B)**, ppRb serine807/81 **(C)**, ppRb serine795 **(D)**, ppRb serine780 **(E)** band intensities, as compared with untreated are shown. **(F)** pRb phosphorylation at serine795 in cultures treated with HIV-MDM is not dependent on NMDA receptor activation. Western immunoblotting of one set of lysates obtained from cultures pre-incubated with 10 μM MK801, 30 minutes before the addition of HIV-MDM or Mock for 16 hours is shown. Fold changes in band intensities over that of the untreated lane are shown. Loading controls were used for normalization (n=3, One-way ANOVA, post-hoc Newman-Keuls, * $p<0.05$ vs. untreated and vs. Mock).

NIH-PA Author Manuscript NIH-PA Author Manuscript NIH-PA Author Manuscript

NIH-PA Author Manuscript

NIH-PA Author Manuscript

NIH-PA Author Manuscript

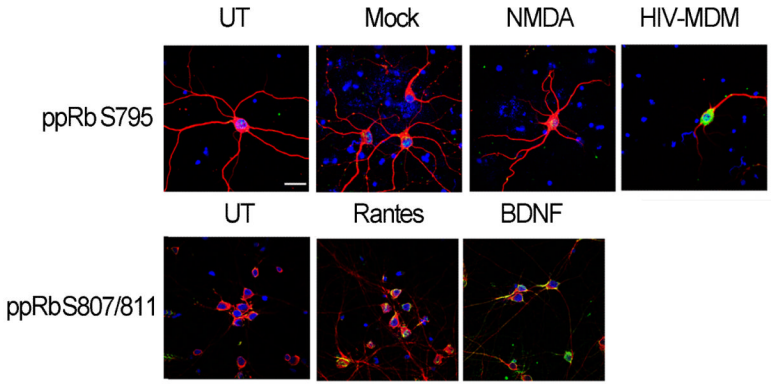

Figure 3. HIV-MDM treatment leads to increased ppRb serine795 in neuronal nuclei, whereas ppRb serine807/811 accumulates in the neuronal cytoplasm in response to BDNF and RANTES treatment *in vitro*.

21 DIV primary rat cortical cultures on coverslips were treated with RANTES, BDNF, NMDA, Mock or HIV-MDM for 1, 2 or 4 hours, followed by immunostaining for ppRb serine795 (green, **A**) or ppRb serine807/811 (green, **B**), MAP2 (red, **A** and **B**), and nuclei (DAPI, blue, **A** and **B**). Images were captured by laser confocal microscopy (n=3). Magnification 600X, scale bar = 20 μm.

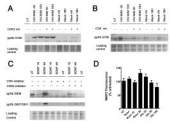

Figure 4. Cyclin dependent kinase 5 (CDK5) preferentially phosphorylates pRb at serine608 and serine807/811 in response to BDNF.

21 DIV primary rat neuroglial cultures were exposed to indicated treatments for 4 and 16 hours in the presence or absence of a 30 min pre-incubation with the CDK5 inhibitor, Roscovitine (10 μM), or general CDK inhibitor, Olomoucine (50 μM). Whole cell lysates were used for immunoblotting with indicated antibodies. Inhibition of CDK5 activity by Roscovitine does not abolish ppRb serine795 formation in cultures treated with HIV-MDM **(A)**, whereas Roscovitine blocks ppRb serine608 and serine807/811 formation by BDNF **(C)**. Olomoucine effectively blocks all ppRb isoforms shown in cultures in response to indicated treatments **(B)** and **(C)**. **D)** Nontoxic Roscovitine and Olomoucine doses were determined by treatment of cultures with the indicated concentrations for 20 hours.

NIH-PA Author Manuscript NIH-PA Author Manuscript NIH-PA Author Manuscript

NIH-PA Author Manuscript

NIH-PA Author Manuscript

NIH-PA Author Manuscript

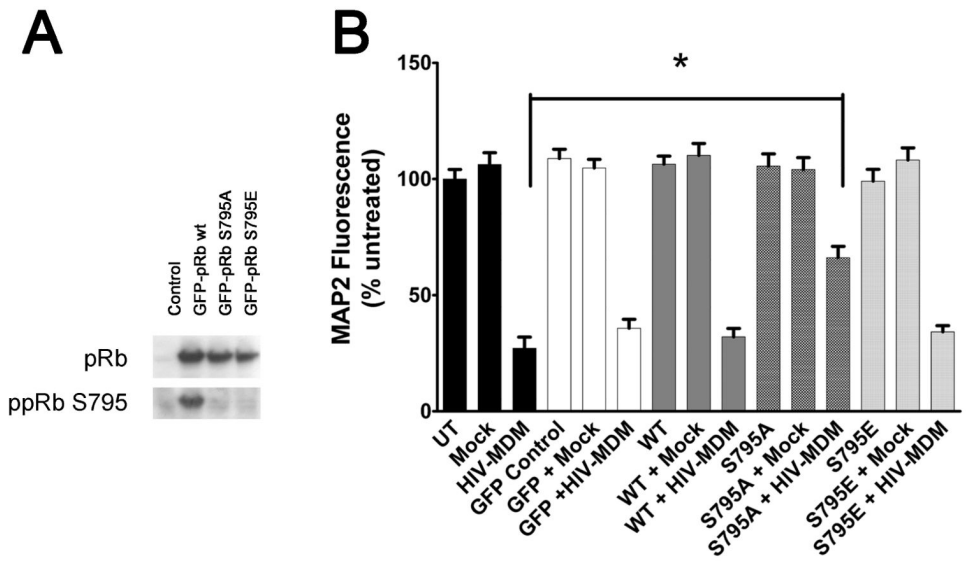

Figure 5. Overexpression of a pRb mutant nonphosphorylatable at serine795 provides protection in neurons treated with HIV-MDM.

A GFP-expressing lentiviral expression system was utilized for overexpression of w.t., ppRb S795A, and ppRb S795E in differentiated neurons *in vitro*. **A)** Overexpression of specific mutants was assessed by immunoblotting using antibodies against total pRb and ppRb S795 in rat neurons 3 days post-infection with lentiviral expression vectors. **B)** Attenuation of HIV-MDM induced MAP2 loss in neurons overexpressing ppRbS795A, as compared with those uninfected, or with those overexpressing w.t. pRb or ppRbS795E. (* $p < 0.05$, One way ANOVA).

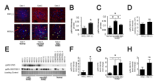

Figure 6. ppRb serine795 levels are increased in HIV-infected brain tissue.

A) and B) Formalin-fixed, paraffin embedded tissue slides from the cases used for immunoblotting were triple-labeled for ppRb serine795 (green), MAP2 (red), and DAPI (blue). Slides were visualized by triple-label immunofluorescent laser confocal microscopy (TLCM) and images taken were quantified for ppRb expression by MetaMorph imaging software. **A)** Representative composite images of 3 cases from HIV(−) and HIV(+) groups show increased ppRb serine795 immunoreactivity in neuronal nuclei of HIV(+) cases. Scale bar = 20 μm. **B)** Quantification shows an increase in ppRb serine795 immunoreactivity is statistically significant in HIV(+) group, as compared with HIV(−) group (Student's t-test, *$p<0.05$). C) ppRb serine795 increase is statistically significant in the less severely compromised group (non-HAD) compared with the more severely compromised group (HAD). The changes in both non-HAD and HAD groups are statistically significant when compared with the neurocognitively normal group (Student's t-test, * $p<0.05$). D) ppRb 807/811 was also examined via TLCM and then quantified using Metamorph. Quantification is show here. **E)** Whole cell tissue lysates from HIV (+) (n=14) and HIV(−) (n=4) cases (table 3) were blotted for all six ppRb forms included in this study. Western blots for ppRb serine795 and ppRb serine807/serine811 are shown. A band for coomassie blue is included to control for equal loading and protein degradation. **E** and **F)** ppRb serine795 levels are increased in HIV(+) cases, as compared with HIV(−) group. **G)** There is a trend towards significance in the increase in ppRb serine795 levels in the HAD group compared with the non-HAD group. **E** and **H)** We did not detect an increase in expression of ppRb serine807/811.

NIH-PA Author Manuscript NIH-PA Author Manuscript NIH-PA Author Manuscript

NIH-PA Author Manuscript
NIH-PA Author Manuscript
NIH-PA Author Manuscript

Table 1

Summary of ppRb antibodies used in this study.

Epitope	Species	Company	Dilution WB	Dilution IFA *in vitro*	Dilution IFA *in vivo*
Threonine249/serine252	rabbit	Biosource	1:1000	1:1000	N/A
Serine608	rabbit	Cell Signaling	1:1000	1:1000	N/A
Serine780	rabbit	Cell Signaling	1:1000	1:1000	N/A
Serine795	rabbit	Cell Signaling	1:1000	1:1000	1:1000
Serine807/811	rabbit	Cell Signaling	1:1000	1:1000	N/A
Threonine821	rabbit	Biosource	1:1000	1:1000	N/A

NIH-PA Author Manuscript
NIH-PA Author Manuscript
NIH-PA Author Manuscript

Table 2

Summary of pRb phosphorylation sites in response to different stimuli in primary rat cortical cultures.

Data is representative of at least 3 experiments.

Site	Subcellular localization	RANTES	BDNF	NMDA	Mock	HIV-MDM
Threonine249/252	**ND**	−	−	−	++	++
Serine608	**ND**	++	+	−	−	−
Serine780	**Cytoplasmic**	+	++	−	++	+
Serine795	**Nuclear**	−	−	−	+	+++
Serine807/811	**cytoplasmic**	+	+	−	+	−
Threonine821	**ND**	+	−	−	++	+

NIH-PA Author Manuscript NIH-PA Author Manuscript NIH-PA Author Manuscript

Table 3

Summary of case data for autopsy tissue obtained from the NNTC.

Data on the HIV status (HIV), Gender, Age in years, post-mortem interval (PMI) in hours, Neurocognitive diagnosis (NeuroCog), and Neuropathological diagnosis (Neuropath Dx) are summarized. Abbreviations include: F – female, HAD – HIV associated dementia, M – Male, MCMD – minor cognitive/motor disorder, and ND – not determined.

Case	HIV	Gender	Age (years)	PMI (hr)	NeuroCog	Neuropath Dx
HIV 1	+	M	35	9.25	HAD	Not HIVE
HIV 2	+	F	34	5	HAD	Not HIVE
HIV 3	+	M	57	5.5	HAD	Not HIVE
HIV 4	+	M	32	14.5	HAD	HIVE
HIV 5	+	M	38	5.5	HAD	HIVE
HIV 6	+	M	32	14	HAD	HIVE
HIV 7	+	M	36	2.5	MCMD	Not HIVE
HIV 8	+	M	37	11.5	MCMD	Not HIVE
HIV 9	+	M	31	8.83	MCMD	Not HIVE
HIV 10	+	M	49	67.33	MCMD	Not HIVE
HIV 11	+	M	42	27.33	MCMD	Not HIVE
HIV 12	+	M	50	21	MCMD	HIVE
HIV 13	+	M	43	unknown	MCMD	HIVE
HIV 14	+	M	46	2.75	Normal	Not HIVE
CONTROL 1	−	M	46	27.65	ND	Control
CONTROL2	−	F	47	19.2	ND	Control
CONTROL3	−	M	40	14.66	ND	Control
CONTROL4	−	F	51	21.75	ND	Control